Effect of rib angle orientation on local mass transfer distribution around sharp 180 deg turn with rib-turbulators mounted in entire two-pass channels

C. Y. Zhao, W. Q. Tao

Abstract The local mass transfer distributions around sharp 180 deg turn with rib-turbulators in a relatively short ($L/D = 4$) two-pass, square channel were determined via the naphthalene sublimation technique. The rib height-to-hydraulic diameter ratio (e/D) was 0.05 and the rib pitch-to-height ratio (p/e) was 10. Experiments were conducted for five attack angles ($\alpha = 90, 45, 60, -45$, and -60 deg), and for three Reynolds numbers (3.0×10^4, 6.0×10^4 and 9.0×10^4). Results show that the rib-roughened wall Sherwood numbers after the turn are higher than those in the turn region, which, in turn, are higher than those before the turn due to the ribs installed in the turn region. While in the previous studies, the ratio Sh/Sh_0 in the turn region was found to be lower than that in the before turn region, because of the absence of rib in the turn region. The rib angle and rib orientation have significant effect on both the local and average Sherwood number ratios. The average Sherwood number ratios (Sh_m/Sh_0) for $\alpha = 60$ deg have the highest values, then comes the case of $\alpha = 45$ deg, and the Sherwood number ratios (Sh_m/Sh_0) for $\alpha = 90$ and -45 deg are the lowest. Correlations for the average rib-roughened wall Sherwood number ratios for the before-turn, in-turn and after-turn segments are provided.

Einfluß der Rippenwinkel-Orientierung auf den lokalen Stoffübergang in einem 180°-Umlenkkanal mit turbulenzerzeugenden Rippen

Zusammenfassung Der lokale Stoffübergang in einem relativ kurzen ($L/D = 4$) 180°-Umlenkkanal mit turbulenzerzeugenden Rippen wurde unter Einsatz der Naphtalin-Sublimationstechnik untersucht. Das Verhältnis von Rippenhöhe zu hydraulischem Durchmesser betrug $e/D = 0,05$ und das von Rippenabstand zu Rippenhöhe $p/e = 10$. Die Experimente wurden mit 5 verschiedenen Anstellwinkeln ($\alpha = 90°, 45°, 60°, -45°, -60°$) und bei drei Reynolds-Zahlen ($3,0 \cdot 10^4$, $6,0 \cdot 10^4$, $9,0 \cdot 10^4$) durchgeführt. Ripppenwinkel und Rippenorientierung zeigten wesentlichen Einfluß auf die lokalen und mitt-leren Sherwood-Zahlen, wobei die höchsten Werte bei $\alpha = 60°$ auftraten; dann folgten immer niedrigere für $45°, 90°$ und $-45°$. Berechnungsgleichungen für mittlere Sherwood-Zahlen in den 3 Segmenten vor, in und nach der $180°$ – Umlenkung werden mitgeteilt.

List of symbols

D	Channel width, also hydraulic diameter
$\tilde{D}$	diffusion coefficient
e	rib height
h	local mass transfer coefficient
m''	local mass transfer rate per unit area
Nu	Nusselt number
P	rib pitch
Pr	Prandtl number
Re	Reynolds number based on channel hydraulic diameter
s	total axial length of each measurement line
Sc	Schmidt number
Sh	local Sherwood number
Sh_m	average Sherwood number on each surface of the test channel
$\overline{Sh}_m$	overall average Sherwood number for the entire rib-roughened wall
Sh_0	Sherwood number for fully developed turbulent tube flow
δ	thickness of the inner (divider) wall
Δt	duration of the test run
x	local distance on each measurement line
X	normalized axial distance of each measurement line, x/s
α	rib angle of attack
v	kinematic viscosity of pure air
ρ_b	bulk naphthalene vapor density in the flow passage
ρ_s	density of solid naphthalene
ρ_w	local naphthalene vapor density at wall

C. Y. Zhao, W. Q. Tao
School of Energy and Power Engineering
Xi'an Jiaotong University
Xi'an, Shaanxi 710049, P.R.C

Correspondence to: W. Q. Tao

1
Introduction

In modern gas turbine blades, as depicted in Fig. 1, cooling air is circulated through internal cooling passages to remove heat from the blade external surfaces that are exposed to high temperature gas flows. A typical cooling passage can be modeled as a straight or a multipass rec-

Turbulence Promoters

Internal Passages
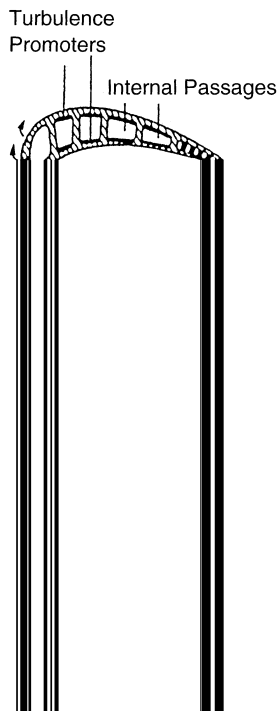
Fig. 1. Schematic diagram of a gas turbine blade

Table 1. Test conditions of the present investigation

Case NO	Angle	P/e	e/D	Re	Configuration
1	90	10	0.05	3.0×10^4	
2	90	10	0.05	6.0×10^4	
3	90	10	0.05	9.0×10^4	
4	45	10	0.05	3.0×10^4	
5	45	10	0.05	6.0×10^4	
6	45	10	0.05	9.0×10^4	
7	60	10	0.05	3.0×10^4	
8	60	10	0.05	6.0×10^4	
9	60	10	0.05	9.0×10^4	
10	-45	10	0.05	3.0×10^4	
11	-45	10	0.05	6.0×10^4	
12	-45	10	0.05	9.0×10^4	
13	-60	10	0.05	3.0×10^4	
14	-60	10	0.05	6.0×10^4	
15	-60	10	0.05	9.0×10^4	

tangular channel with a pair of opposite rib-roughened walls. In a straight rib-roughened channel, the effects of the turbulators' configuration (such as rib height, spacing, and angle), the flow channel aspect ratio, and the flow Reynolds number on the distributions of the local heat transfer and pressure drop have been extensively studied [1]–[4].

In a multipass rib-roughened channel, Boyle [5] studied the effect of the sharp 180 deg turn on the local heat transfer coefficient in a two-pass square channel roughened by transverse ribs. Since the test channels in his study were sparsely instrumented with thermocouples, the detailed distributions of the local heat transfer around the sharp 180 deg turn were not determined. With the naphthalene sublimation technique, Han [6] studied the effect of the sharp 180 deg turn on the distributions of the local mass transfer coefficient around the turn region in a two-pass square channel roughened by the transverse ribs ($\alpha = 90$), and Chandra [7] investigated the effect of the rib angle on the local heat transfer distribution in a two-pass rib-roughened channel.

It should be noted that in almost all of the previous studies, there is no rib in the turn region, so the local Sherwood number ratio Sh/Sh_0 in the after-turn region is lower than that of the before-turn. In addition, most of the previous studies consider the fully developed flow and heat transfer, while, some practical applications include the developing region. Even for those studies with a relatively short duct, the values of L/D are usually greater than 8–10. Sometimes, however, a much shorter duct may be encountered in practice.

In this work, the turbulent air flow in a two-pass rib-roughened square duct with $L/D = 4$ was investigated. The rib attack angles were $90°, 45°, 60°, -45°$ and $-60°$.

The detailed distribution of the mass transfer coefficient around sharp 180 deg turn with rib turbulators was measured via the naphthalene sublimation technique for three Reynolds number (3.0×10^4, 6.0×10^4, 9.0×10^4). Emphasis was placed on determining the effects of rib angle and rib orientation on mass transfer. The top, bottom, outer and inner (divider) walls of the test channel were all coated with naphthalene, and steel rib-turbulators were attached to the top and bottom walls in the before- and after-turn region, and in the turn region as well. The rib pitch-to-height ratio (p/e) was 10, and the rib height-to-hydraulic diameter ratio (e/D) was 0.05. A total of fifteen test runs were performed. The test conditions of the runs are given in Table. 1.

2
Experimental apparatus and procedure
The test apparatus consisted of a test section, a Pilot – tube, a gate valve, and a centrifugal blower.

Figure 2 is a schematic diagram of the test section – a two-pass channel with a 5.0 cm square cross section. The top, bottom and outer walls of the channel were constructed of 0.8 cm thick aluminum plates. The inner (divider) wall was made of two 0.5 cm thick aluminum plates, bonded together back to back with double side tape. The turn clearance was equivalent to the channel width (5.0 cm). The ratio of the before-turn (and also the after-turn) channel length to the channel width, L/D, and the ratio of the divider wall thickness to the channel width, δ/D, were kept at 4 and 0.2, respectively.

All the aluminum plates that made up the walls of the test channel were hollowed out and filled with naphthalene by casting against a highly polished stainless steel plate. As a result, all the interior surface of the test channel were
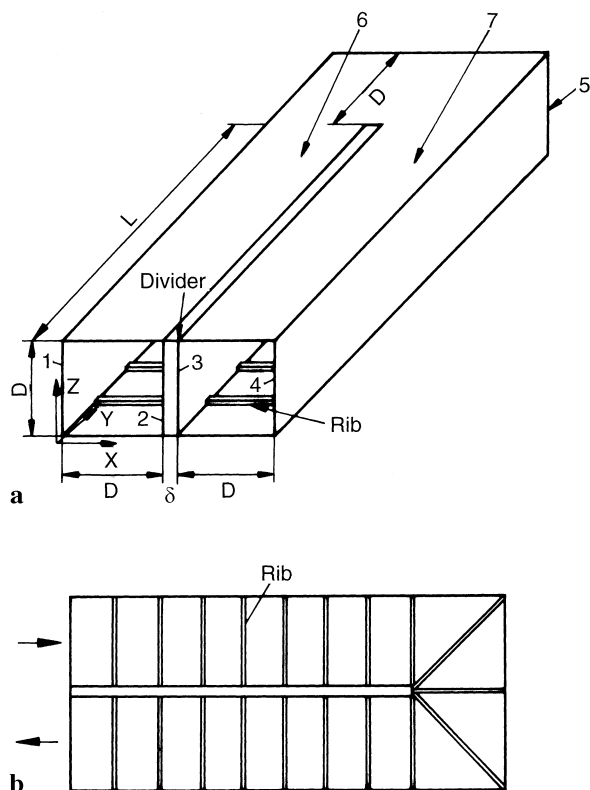
Fig. 2a,b. Configuration of the duct. **a** Pictorial view; **b** top view with rib of $\alpha = 90°$

Fig. 3. Top-plane view with three measurement lines

smooth naphthalene surfaces. Steel ribs with a 2.5 mm square cross section were glued periodically to the top and bottom naphthalene surfaces (including the turn region).

An entrance section was attached to the inlet of the test section to provide a relatively even flow entrance condition. During a test run, air from the naphthalene-free laboratory was drawn through the test section and conducted to the outside of the building.

The most important part of the present experiment is the instrumentation used to measure the depth change of the naphthalene surfaces. Highly localized measurements of the mass transfer rates were implemented with the aid of a stylus-type gauge. It was a linear variable differential transformer that could provide 0.2 mm linear range and 0.5×10^{-3} mm resolution. This resolution was about two orders of magnitude smaller than the operating range of the measured naphthalene sublimation. The data of the surface profile before and after data-run were recorded by a HP3054 data acquisition system. The change in naphthalene depth of each surface was determined by differencing the two measured surface elevations at given postion. The elevation measurement stations are schematically shown in Fig. 3. The total sublimation amount of each surface was then obtained by numerical integration. In addition, the total sublimation amount of surface 5 during a data run was also determined with an analytical balance having a resolution of 0.0001 g and a capacity of 200 g. The weights of other surfaces were beyond the analytical balance capacity, hence, were not measured. It was required that the deviation of the total sublimation
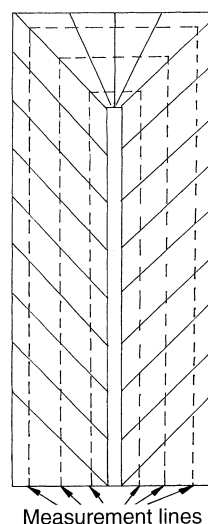
amount of surface 5 from numerical integration and weighing should be less than 8%.

After all the naphthalene plates were prepared, they were tightly sealed individually in plastic bags to prevent sublimation. They were then left in the laboratory for about 8 hour to attain thermal equilibrium. Before a test run, the surface contours of all the naphthalene plates were measured and recorded. The ribs were glued to the appropriate positions of the naphthalene surface. The test section was then assembled and attached to the test rig. To initiate the test run, the blower was switched on for air to flow through the test channel at a predetermined rate. During the test run, the temperature, and the atmospheric pressure were recorded periodically. At the completion of the test run, the contours of the naphthalene surfaces were measured again.

Supplementary tests were conducted to determine the mass losses from the various naphthalene surfaces due to natural convection while the surface contours were being measured and the ribs were being glued onto the appropriate naphthalene surfaces. The total mass loss by natural convection was no more than 3 percent of the total mass transfer during any test run. In calculating the local Sherwood numbers, these losses of mass from the various naphthalene surfaces were taken into account accordingly.

3
Data reduction

3.1
Local Sherwood number
The local mass flux at any measurement point is calculated by the following equation

$$m'' = \rho_s \Delta z / \Delta t \tag{1}$$

where Δz is the measured change of elevation at the measurement point and Δt is the duration of the test run.

The local mass transfer coefficient is defined as

$$h_m = m'' / (\rho_w - \rho_b) \tag{2}$$

where the bulk naphthalene vapor density was obtained by the accumulative mass transferred from the naphthalene surfaces to the air-stream divided by the air volumetric flow rate. The local vapor density was determined by the perfect gas law and the vapor pressure relationship [8].

$$\rho_w = P_w/(R_v T_w) \tag{3}$$

$$\log P_w = A - B/T_w \tag{4}$$

where A, and B are given by Sogin [8].

The local Sherwood number is defined as

$$Sh = hD/\tilde{D} = hD/(v/Sc) \tag{5}$$

The Schmidt number Sc should not be considered a constant, rather, it is a function of the temperature. According to the Goldstein and Cho [9], the Schmidt number can be determined by

$$Sc = 2.28\left(\frac{T}{298.16}\right)^{-0.1526} \tag{6}$$

Based on the heat and mass transfer analogy [8], the local Sherwood number is converted to the corresponding local Nusselt number as

$$Nu = (Pr/Sc)^{0.4} Sh \tag{7}$$

The Nusselt number for fully developed turbulent tube flow correlated by McAdams

$$Nu_0 = 0.023 Re^{0.8} Pr^{0.4} \tag{8}$$

was taken as the reference for comparison. By combining Eqs. (5), (7) and (8), the experimentally determined local Sherwood number is normalized as follows:

$$Sh/Sh_0 = (hD/\bar{D})/(0.023 Re^{0.8} Pr^{0.4}(Sc/Pr)^{0.4}) \tag{9}$$

3.2
Uncertainties in data reduction
For a 0.56 °C variation in the naphthalene surface temperature, there was a 6 percent change in the local naphthalene vapor density. In the present study, the variation of temperature for any test run was never more than 0.35 °C. Therefore, the uncertainties in the local vapor density (ρ_w) calculations caused by the reference temperature were relatively small (about 2%).

Since the surface contours were measured at discrete points along three axial lines on the naphthalene surfaces as shown in Fig. 3, errors were introduced into the calculation of the bulk naphthalene vapor densities (ρ_b) that were determined from the accumulative mass transferred into the airstream. The values of the bulk vapor density were small, with a maximum of about 10 percent of ρ_w. In addition, the uncertainty introduced by Eq. (4) has to be added (about 3–4%). All the factors being considered, the maximum uncertainty in the calculations of ($\rho_w - \rho_b$) was estimated to be 7 percent. The uncertainties in the calculations of the density of solid naphthalene, ρ_s, in the elevation measurement, Δz, and in the duration of the test run, Δt, were estimated to be 1.0, 3.5, and 2.0 percent, respectively. The maximum uncertainty of the local Sherwood number was determined to be about 8 percent by the uncertainty estimation method of Kline and McClintock [10].

4
Experimental results and discussion
In this section, the axial distributions of a normalized Sherwood number ratio, Sh/Sh_0, are presented (Eq. (9)). For each set of data, the Sherwood number ratios along the inner line, the center line and the outer line (Fig. 3) on the top wall (i.e, rib-roughened wall) are plotted separately.

4.1
Effect of rib angle
The distributions of the top-wall Sherwood number ratio for $\alpha = 90$ deg and $Re = 3.0 \times 10^4$ are shown in Fig. 4. The periodic nature of the distributions is evident. In the before-turn region, the Sherwood number ratios attain their maximum values at the points of flow reattachment after each rib, which occur slightly upstream of the midpoints between two adjacent ribs. The variations of the Sherwood number ratio in the spanwise direction (see the three panels of Fig. 4) are very small compared with the axial variations. In the turn region, for ribs are also installed, the Sh/Sh_0 values are higher than those of the before-turn region, and the axial Sh/Sh_0 distribution also settles into a periodic pattern, which is different from the previous studies (there was no rib in the turn region in the previous studies). After the turn region, due to the sharp turn effect, the Sherwood number ratios along the outer line are slightly higher than those along the center line, which, in turn, are slightly higher than those along the inner line. In general, the Sherwood number ratios after the turn are
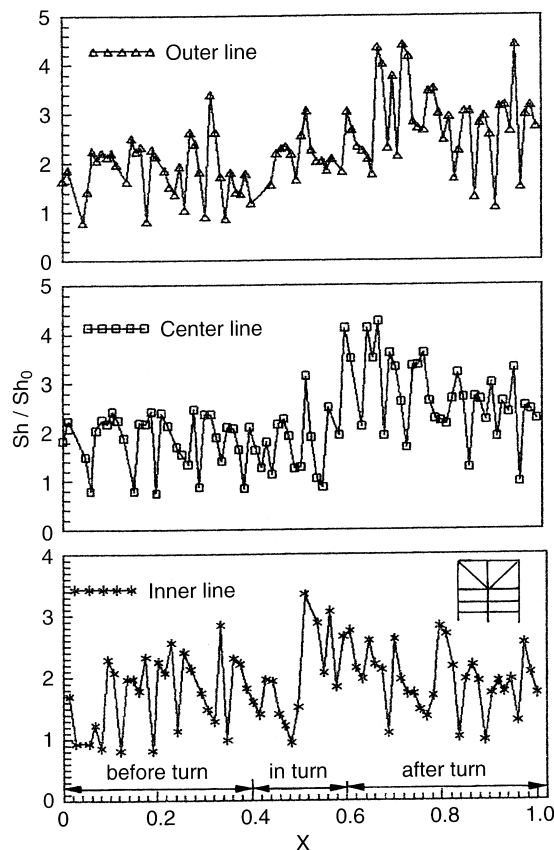

Fig. 4. Local Sherwood number distribution for $\alpha = 90$ deg and $Re = 3.0 \times 10^4$
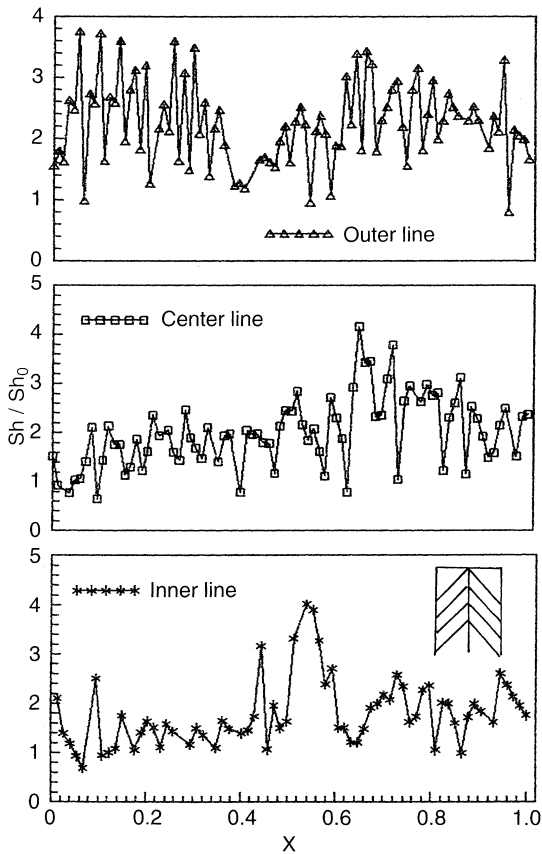
Fig. 7. Local Sherwood number distribution for $\alpha = -45$ deg and $Re = 3.0 \times 10^4$

Fig. 8. Local Sherwood number distribution for $\alpha = -60$ deg and $Re = 3.0 \times 10^4$

The top-wall Sh/Sh_0 distribution for $\alpha = -60$ deg and $Re = 3.0 \times 10^4$ is shown in Fig. 8. We can see that the Sh/Sh_0 distributions are quite similar to those for $\alpha = -45$ deg.

4.3
Average Sherwood number and correlations
For all the cases studied, the local Sherwood number ratios for individual surfaces of the channel walls before the turn, in the turn, and after the turn were averaged. In Fig. 9, the average Sherwood number ratios (Sh_m/Sh_0) are plotted as functions of the Reynolds number. Fig. 9(a) shows that in the before-turn top-wall values of Sh_m/Sh_0 for $\alpha = -60$ deg are the highest, and the Sh_m/Sh_0 for $\alpha = 90$ deg are the lowest, which supports the finding provided by Chandra et al [7]. In the turn region, the Sh_m/Sh_0 values for $\alpha = 60$ deg have the highest values, while those of $\alpha = -45$ and -60 deg are relatively low (Fig. 9(b)). After the turn region, the Sh_m/Sh_0 ratios have the highest values for $\alpha = 60$ deg, and have the lowest values for $\alpha = -60$ deg (Fig. 9(c)). In general, the after-turn Sh_m/Sh_0 values are always higher than the corresponding in-turn values, which, in turn, are higher than the before-turn values.

The overall average Sherwood number ratios for the entire top wall $\overline{Sh}_m/Sh_0$ of the five rib angles studied are plotted versus the flow Reynolds number in Fig. 9(d). It can be seen that the overall $\overline{Sh}_m/Sh_0$ ratios have the

highest values for $\alpha = 60$ deg and have relatively low values for $\alpha = -45$ deg and for $\alpha = 90$ deg.

The average Sherwood number ratios for the various segments of the channel walls were found to be correlated well with the Reynolds number and the rib angle by the following equation:

$$Sh_m/Sh_0 = aRe^b(\alpha/90)^c \qquad (10)$$

To qualitatively account for the rib orientation effect on Sh_m/Sh_0 ratios, the Sh_m/Sh_0 for $\alpha = 90, 45$ and 60 and for $\alpha = 90, -45$ and -60 deg are grouped separately. The numerical values of a, b and c coefficients are listed in Table. 2. Equation (10) correlates all of the Sh_m/Sh_0 data of the present investigation within ± 8 percent.

5
Conclusions
The experimental investigation reported here has provided the local mass transfer coefficient data around sharp 180 deg turn with rib turbulators in a relatively short entire two-pass channel. The main findings of the investigation are as follows:
1. The rib orientation has significant effects on the local heat/mass transfer distributions. These effects include: (a) In the before-turn region, the rib-roughened local Sherwood numbers near the inner wall for $\alpha = 45$ and 60 deg are higher than those near the outer wall, while for the case of $\alpha = -45$ and -60 deg, the situation is
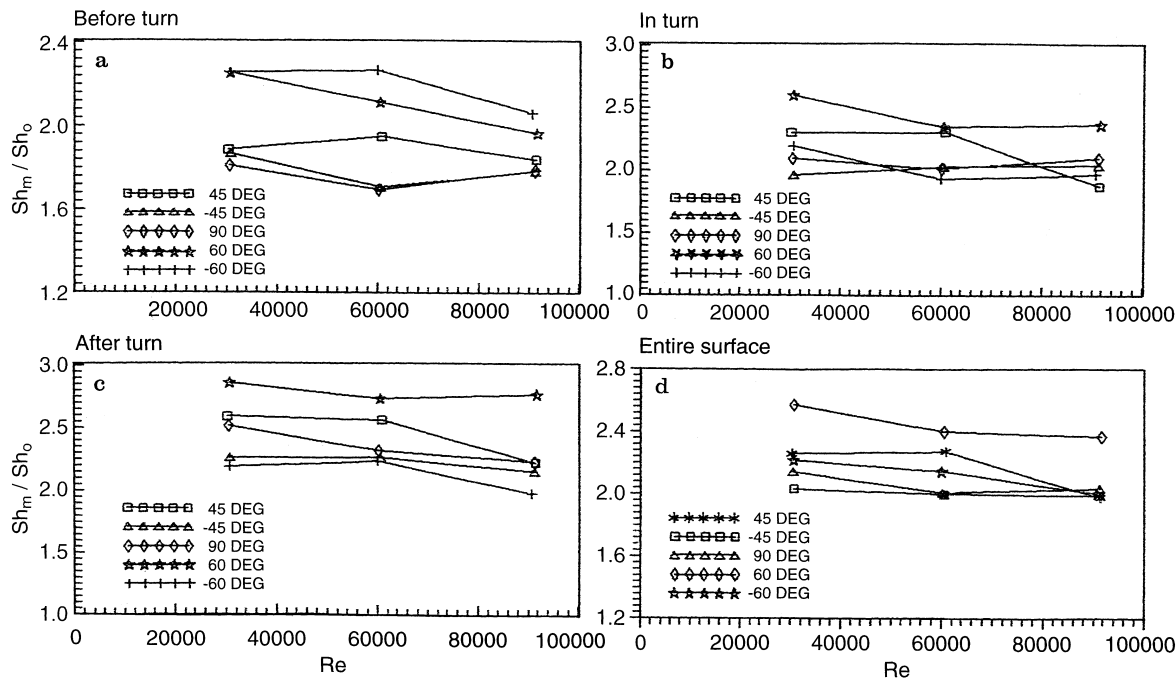
Fig. 9a-d. Average Sherwood number vs. Reynolds number. a Before turn; b in turn; c after turn; d entire surface

just the opposite. The spanwise variations of the top-wall local Sherwood number for $\alpha = 90°$ case are insignificant.

(b) In the after-turn region, for the cases of $\alpha = 45$ and 60 deg, the top-wall local Sherwood numbers near the outer wall are higher than those near the inner wall. For $\alpha = -45$ and -60 degree, however, the spanwise variations of the rib-roughened wall are not so significant. This difference is the outcome of the complicated interaction between the main flow and the secondary flow in the after-turn region.

(c) For the five orientation studied, the average top-wall Sherwood number for $\alpha = -60$ deg is the highest for the before-turn region, while in the after-turn region, it is the lowest. For the case of $\alpha = 60$ deg, the average top-wall Sherwood number before the turn is the second. While it becomes the highest for both in-turn and after-turn regions.

(d) For the case of $\alpha = 60$ deg, the overall average Sherwood number of the entire rib-roughened wall is the highest among the all cases studied, and that of $\alpha = 45$ deg takes the second, for $\alpha = -45$ and 90 deg, the overall Sherwood numbers are in the lowest position.

2. For all rib orientations studied, the top-wall local Sherwood numbers in the turn-region are higher than those of the before-turn due to the ribs installed in this region.

3. The average Sherwood number ratios, Sh_m/Sh_0 of the entirely ribbed-wall are slightly decrease with increasing Reynolds number.

4. The average Sherwood number ratios for the before-turn, in-turn and after-turn regions can be well correlated by Eq. (10).

Table 2. Coefficients a, b and c in Eq. (10)

α	Region	a	b	c
90, 45	before turn	2.200	−0.020	−0.103
as a	in turn	5.373	−0.087	−0.057
group	after turn	8.654	−0.119	−0.062
90, 60	before turn	3.877	−0.072	−0.439
as a	in turn	3.569	−0.050	−0.404
group	after turn	5.235	−0.073	−0.421
90, −45	before turn	2.641	−3.685	−0.018
as a	in turn	1.778	0.000	0.040
group	after turn	5.478	−0.077	0.081
90, −60	before turn	2.988	−0.048	−0.537
as a	in turn	3.897	−0.058	0.047
group	after turn	6.841	−0.098	0.242

References

1. **Han, J. C.:** Heat transfer and friction in channels with two opposite rib-roughened walls. ASME Journal of Heat Transfer, 106 (1984) 774–781
2. **Han, J. C.; Park, J. S.; Lei, C. K.:** Heat transfer enhancement in channels with turbulence promoters. ASME Journal of Engineering for Gas Turbines and Power 107 (1985) 629–635
3. **Han, J. C.:** Heat transfer and friction characteristics in rectangular channel with rib turbulators. ASME Journal of Heat Transfer. 110 (2) (1988) 321–328
4. **Han, J. C.; Park, J. S.:** Developing heat transfer in rectangular channels with rib turbulators. International Journal of Heat and Mass Transfer 31 (1) (1988) 183–195
5. **Boyle, R. J.:** Heat transfer in serpentine passages with turbulence promoters. ASME paper No. 84-HT-24 (1984)
6. **Han, J. C.; Chandra, P. R.; Lau, S. C.:** Local heat/mass transfer distributions around sharp 180 turns in two-pass smooth and rib-roughened channels. ASME Journal of Heat Transfer 110 (1) (1988) 91–98
7. **Chandra, P. R.; Han, J. C.; Lau, S. C.:** Effect of rib angle on local heat/mass transfer distribution in a two-pass rib roughened Channel. ASME Journal of Turbomachinery 110 (1988) 233–241

8. **Sogin, H. H.:** Sublimation from disks to air stream flowing normal to their surfaces. Trans ASME, 80 (1958) 61–69

9. **Goldstein, R. J.; Cho, H. H.:** A review of mass (heat) transfer measurements using napthalene sublimation. Experimental Heat Transfer, Fluid Mechanics and Thermodynamics (1993)

10. **Kline, S. J.; McClintock, F. A.:** Describing uncertainties in single sample experiments. Mechanical Engineering 75 (1953) 3–8

11. **Han, J. C.; Zhang. P.:** Effects of rib-angle orientation on local mass transfer distribution in a three-pass rib-roughened channel. ASME Journal of Turbomachinery 113 (1991) 123–130